International Journal of Nanomedicine

Dovepress
open access to scientific and medical research

Open Access Full Text Article

ORIGINAL RESEARCH

A Novel Liposomal S-Propargyl-Cysteine: A Sustained Release of Hydrogen Sulfide Reducing Myocardial Fibrosis via TGF-β1/Smad Pathway

This article was published in the following Dove Press journal:
International Journal of Nanomedicine

Ba Hieu Tran,[1–3] Ying Yu,[1,4] Lingling Chang,[1] Bo Tan,[5] Wanwan Jia,[1] Ying Xiong,[1] Tao Dai,[1] Rui Zhong,[1] Weiping Zhang,[6] Van Minh Le,[7] Peter Rose,[8] Zhijun Wang,[1,2] Yicheng Mao,[1,*] Yi Zhun Zhu[1,2,*]

[1]School of Pharmacy, Fudan University, Shanghai, People's Republic of China; [2]School of Pharmacy, Macau University of Science and Technology, Taipa, Macau; [3]Institute of Biomedicine and Pharmacy, Vietnam Military Medical University, Hanoi, Vietnam; [4]Department of Cardiology, Xinhua Hospital, Shanghai, People's Republic of China; [5]Department of Clinical Pharmacology, Shuguang Hospital Affiliated to Shanghai University of Traditional Chinese Medicine, Shanghai, People's Republic of China; [6]Department of Hematology, Institute of Hematology of PLA, Changhai Hospital, Shanghai, People's Republic of China; [7]NTT Institute of Hi-Technology (NIH), Nguyen Tat Thanh University, Ho Chi Minh City, Viet Nam; [8]School of Biosciences, University of Nottingham, Loughborough, LE12 5RD, UK

*These authors contributed equally to this work

Correspondence: Yicheng Mao; Yi Zhun Zhu
School of Pharmacy, Fudan University, 826 Zhangheng Road, Shanghai 201203, People's Republic of China
Tel +86 21 5198 0041; +853 8897 2880
Fax +853 2882 3575
Email maoyc@fudan.edu.cn; yzzhu@must.edu.mo

Purpose: S-propargyl-cysteine (SPRC; alternatively known as ZYZ-802) is a novel modulator of endogenous tissue H_2S concentrations with known cardioprotective and anti-inflammatory effects. However, its rapid metabolism and excretion have limited its clinical application. To overcome these issues, we have developed some novel liposomal carriers to deliver ZYZ-802 to cells and tissues and have characterized their physicochemical, morphological and pharmacological properties.

Methods: Two liposomal formulations of ZYZ-802 were prepared by thin-layer hydration and the morphological characteristics of each liposome system were assessed using a laser particle size analyzer and transmission electron microscopy. The entrapment efficiency and ZYZ-802 release profiles were determined following ultrafiltration centrifugation, dialysis tube and HPLC measurements. LC-MS/MS was used to evaluate the pharmacokinetic parameters and tissue distribution profiles of each formulation via the measurements of plasma and tissues ZYZ-802 and H_2S concentrations. Using an in vivo model of heart failure (HF), the cardio-protective effects of liposomal carrier were determined by echocardiography, histopathology, Western blot and the assessment of antioxidant and myocardial fibrosis markers.

Results: Both liposomal formulations improved ZYZ-802 pharmacokinetics and optimized H_2S concentrations in plasma and tissues. Liposomal ZYZ-802 showed enhanced cardioprotective effects in vivo. Importantly, liposomal ZYZ-802 could inhibit myocardial fibrosis via the inhibition of the TGF-β1/Smad signaling pathway.

Conclusion: The liposomal formulations of ZYZ-802 have enhanced pharmacokinetic and pharmacological properties in vivo. This work is the first report to describe the development of liposomal formulations to improve the sustained release of H_2S within tissues.

Keywords: liposome, S-Propargyl-cysteine, SPRC, ZYZ-802, hydrogen sulfide, heart failure, myocardial fibrosis, TGF-β1/Smad pathway

Introduction

Over the last decade, great strides have been made in our understanding of the biological and physiological significance of hydrogen sulfide gas (H_2S) in mammals.[1–3] Importantly, this molecule is regarded as the third gasotransmitter alongside carbon monoxide and nitric oxide. In the cells and tissues of our bodies, H_2S is produced by the enzymes cystathionine β-synthase (CBS), cystathionine γ-lyase (CSE), and 3-mercaptopyruvate sulfur transferase (3-MST).[4] Within the cardiovascular system, H_2S production, via the catabolism of cysteine by the enzyme CSE, is reported to act as a cytoprotectant against oxidative stress and has distinct functions in inflammatory and apoptotic signaling.[5,6]

© 2019 Tran et al. This work is published and licensed by Dove Medical Press Limited. The full terms of this license are available at https://www.dovepress.com/terms.php and incorporate the Creative Commons Attribution – Non Commercial (unported, v3.0) License (http://creativecommons.org/licenses/by-nc/3.0/). By accessing the work you hereby accept the Terms. Non-commercial uses of the work are permitted without any further permission from Dove Medical Press Limited, provided the work is properly attributed. For permission for commercial use of this work, please see paragraphs 4.2 and 5 of our Terms (https://www.dovepress.com/terms.php).

Moreover, roles for H_2S gas production in vasorelaxation,[7] the stimulation of angiogenesis,[8–10] and protective functions in myocardial ischemia,[11,12] atherosclerosis,[13] anemia,[14,15] hypertension,[16] hypoxia[17] and heart failure[18] have been reported.

Owing to the important roles for this gas in many physiological processes, a variety of natural and synthetic donor molecules have been developed to allow for the manipulation of H_2S gas within tissues.[19,20] Of the many donor molecules described, one of the most widely characterized, is S-propargyl-cysteine (SPRC) alternatively known as ZYZ-802. ZYZ-802 is a structural analogue of S-allylcysteine (SAC), a constituent of garlic with known cardioprotective effects.[21] To date, ZYZ-802 has been shown to be protective in models of hypoxia/reoxygenation (H/R) injury,[22] ischemic reperfusion injury,[23] in heart failure (HF)[24] and in angiogenesis.[25] One of the key mechanisms responsible for these effects is the ability of ZYZ-802 to increase the expression and activity of CSE protein and to increase endogenous H_2S concentrations in animal tissues. Therefore, ZYZ-802 could serve as a useful tool to allow for the manipulation of H_2S gas in vitro and in vivo. In spite of this, ZYZ-802 suffers from one major drawback, that of its rapid metabolism and elimination in animal tissues.[26] This fact alone limits any clinical application for this molecule and as such new delivery strategies are needed to improve the pharmacokinetic profile of this molecule.[27]

Lately, liposomes have been shown as useful delivery vehicles for drugs with poor physiochemical characteristics like poor solubility or poor pharmacokinetics traits.[28] These nanoparticles are formed by the self-assembly of phospholipid molecules and can be used as carriers for the delivery of therapeutic molecules.[29] The manipulation of these carrier systems via the incorporation of polymers such as polyethylene glycol (PEG) or the incorporation of targeting ligands such as antibody can prolong circulation times, reduced immunogenicity and provide targeted delivery of drug-like molecules to target tissues. Cationic liposomes have been used as an excellent delivery carrier for antitumor drugs, and the cationic charge on the liposomal surface facilitates the intracellular uptake of the carrier via the electrostatic interaction with the anionic charge of cancer cell membrane.[30] Temperature-sensitive liposomes have been shown to be effective for tumor-suppression in association with hyperthermia because of their superior biodegradability, drug encapsulation capability, and sharp response to ambient temperature change.[31] Recently, the development of heart-targeted liposomal carriers is promising to lower the incidence of heart diseases.[32] Anti-P-selectin conjugated immunoliposomes containing VEGF could significantly improve vascularization and cardiac function based on the overexpression of P-selection in the infarcted myocardium.[33] PEGylated liposomal adenosine showed to enhance the cardioprotective effects of adenosine against I/R injury and to reduce its unfavorable hemodynamic effects.[34]

In this study, we have developed two liposomal carriers of ZYZ-802 and characterized their physicochemical, morphological and pharmacological properties. We expected that these two liposome formulations of ZYZ-802 could realize sustained release of ZYZ-802 both in vitro and in vivo, which further could increase the corresponding level of H_2S in heart and improve the cardioprotective effects of ZYZ-802 against hypoxia. In vivo, one of the optimized liposomal ZYZ-802 was applied to a rat HF model with left coronary artery ligation, which was supposed to be effective for therapeutic efficacy based on the in vitro and pharmacokinetic study result. The TGF-β1/Smad pathway and its downstream molecules were evaluated for the exploration of the anti-myocardial fibrosis effect of DP-ZYZ-802.

Materials and Methods

Animal

Male Sprague-Dawley rats weighing 200–220 g (8–10 weeks old) were used in our previous studies in specific pathogen-free (SPF) facility[24,25,27] and were obtained from the Joint Ventures Sipper-BK Experimental Animal Co (Shanghai, China) in the current study. Animals were maintained under SPF conditions with stable room temperatures (24±1°C) and humidity levels (50–60%), and a 12 hrs light-dark cycle. Each polycarbonate animal cages contained six rats with wooden chips as bedding that was changed daily. All animals had access to food and water with body weights were recorded daily throughout the course of all experiments. In each experiment, rats were divided upon arrival into groups using restricted randomization so that average body weights were similar between the groups. The animals were treated humanely, all surgery was performed under anesthesia of 1.5% inhalational isoflurane and all efforts were made to minimize animal suffering and the animal numbers. All work involving animals was approved by the Department of Animal Care and Use Committee of Fudan University, and all experiments were conducted according to the Guide for the Care and Use of Laboratory Animals of the

Ministry of National Health and Family Planning of People's Republic of China. Animal studies were carried out in compliance with the current NIH guidelines.[35]

Chemicals and Reagents

ZYZ-802 was synthesized by our laboratory as previously described.[23] Hydrogenated soy phosphatidylcholine (HSPC), cholesterol (Chol), poly (ethylene glycol) (MW ~2,000 Da)-disteroylphosphatidylethanolamine (PEG-DSPE) were purchased from NFC (Japan). Trichloromethane, dicetylphosphate (DP) and stearylamine (SA) were purchased from Sigma-Aldrich (St Louis, MO, USA).

Design and Preparation of Liposomal ZYZ-802

Two formulations of liposomal ZYZ-802 were prepared using thin-layer hydration. Briefly, two liposomal carriers were synthesized and had the following lipid composition, HSPC: Chol: DSPE-PEG: SA (molar ratio = 55: 35: 3: 7) or, HSPC: Chol: DSPE-PEG: DP (molar ratio = 55: 35: 3: 7). Both were dissolved in trichloromethane and these represented SA-ZYZ-802 and DP-ZYZ-802 respectively. The organic solvent was removed under vacuum using a rotary evaporator at 40°C and the homogenous lipid film obtained further dried under a vacuum overnight. 20 mM ZYZ-802 in PBS was added to each lipid film in a 65°C water bath and shaken for 2 hrs to form a liposomal suspension. Finally, liposomal carriers were prepared via a high-pressure micro-jet (Nano DeBEE, B.E.E. International, Inc, USA) maintained at 4°C to form unilamellar liposomal particles containing ZYZ-802 having a diameter of 200 nm. Thereafter, the liposomes were dialyzed against PBS for 4 hrs using a Spectra/Por® with a molecular weight cut-off of 10 KDa (Float-A-Lyzer G2; Spectrum Laboratories, Inc, USA) to remove any non-encapsulated ZYZ-802.

Characterization of Liposomal ZYZ-802

An ultrafiltration centrifugation method was employed to determine the entrapment efficiency (EE) of LP-ZYZ-802. LP-ZYZ-802 was divided into two 1 mL samples. The first sample was diluted (10 ×) using distilled water in an ultrafiltration tube (Slide-A-Lyzer, MWCO: 10KDa; Thermo Scientific, USA) and centrifuged at 4000 rpm/10mins. The bottom liquid was collected and analyzed by HPLC to determine the concentration of ZYZ-802 with this serving as a measurement reflective of the C_{free} fraction. The remaining 1 mL aliquot was diluted (10 ×) with methanol to rupture the liposomal carriers and the concentration of ZYZ-802 determined by HPLC. This sample represented the C_{total} value. Entrapment efficiency was calculated according to the following calculation:

$$EE\% = 100\% \times (C_{total} - C_{free})/C_{total}$$

Five independent batches of liposome were evaluated with the mean EE (%) ± standard deviation.

The size distribution of liposomes was determined by dynamic light scattering (ZEN5600, Malvern Instruments Limited, UK). Five independent batches of each liposome formulation were evaluated to calculate the mean diameter by volume ± standard deviation values. The zeta-potentials were measured using a ZetaPALS zeta-potential analyzer (ZEN5600, Malvern Instruments Limited, UK). In brief, liposomes from five independently produced batches were diluted in deionized water. The Smoluchowski model was used to calculate the zeta-potential for each liposomal carrier and the results expressed as the mean ± standard deviation. Key morphological characteristics for both SA-ZYZ-802 and DP-ZYZ-802 were observed using a transmission electron microscope (JEM −2100F, JEM Japan). For the analysis of liposomes, suspensions were absorbed on to a carbon-coated copper grid and place upon some filter paper. The grids were air-dried, visualized, and photographed. For the stability studies, five independent batches of liposome were stored and sealed in sterile vials at 4°C for 30 and 60 days. Thereafter, samples were taken out from the vials for characterization including particle size, and entrapment efficiency evaluation. The stability of liposomal ZYZ-802 was assessed in line with the original values before storage.

For drug release studies, an in vitro model was used to determine the retention of ZYZ-802 in both liposome carriers. In essence, LP-ZYZ-802 was dialyzed against PBS in dialysis tubing (Float-A-Lyzer G2; MWCO 10K, Spectrum Laboratories, Inc. USA) at room temperature. Samples remaining in the dialysis tube were collected at different time points (0, 0.5, 1, 2, 4, 6, 8, 10, 12, 24, 30 and 36 hrs), and the liposomes ruptured using methanol. The concentration of ZYZ-802 was then measured in each fraction using HPLC and the release rates calculated.

Pharmacokinetic Studies

The plasma pharmacokinetic profiles of free ZYZ-802, DP-ZYZ-802 and SA-ZYZ-802 were evaluated in male SPF Sprague-Dawley rats (8–10 weeks, weighing 200–220g)

and these animals were fasted for 12 hrs before and 3 hrs after dosing. These animals were weighed and followed a restrict randomization to ensure the average weights of rats in each group were similar. In groups of six, rats were intravenously injected with ZYZ-802 (10 mg/kg body weight) via the tail vein and the plasma concentrations of ZYZ-802 determined across the time points (0.25, 0.5, 1, 2, 4, 6, 8, 10, 12, 24, 30, 36 and 48 hrs) by collecting tail vein blood samples (50 μL). ZYZ-802 was extracted from the plasma samples and measured using LC-MS/MS as previously reported.[36] In brief, chromatographic analysis was performed on an Agilent 1200 Series HPLC system (Agilent Technologies, Palo Alto, CA, USA) equipped with a column (150mm×4.6mm i.d. with 5 μm particles, Shiseido, Japan) which contained C18 bonded silica particles and sulfonic acid cation-exchange particles. The mobile phase was composed of acetonitrile/ammonium acetate buffer (10 mM, pH 4): 30/70 (v/v). The mass spectrometer was operated in positive ion mode using an AB 4000Q TRAP tandem mass spectrometer. Quantification was performed by multiple reaction monitoring (MRM) of the transitions of m/z 160.0→143.0 for SPRC and 178.1→160.9 for S-butyl-cysteine (IS). The method was validated according to the Guidelines for Bioanalytical Method Validation of the Food and Drug Administration (FDA). DAS2.1 (M002-V2.1, Data Analysis System, DAS for PK, Mathematical Pharmacology Professional Committee of China, Shanghai, China). Absolute bioavailability (F) was determined for each dose according to the following equation: F (%) $=AUC_{0-t}$ (i.g.)/AUC_{0-t}(i.v.) ×100 (AUC_{0-t}, estimated using linear trapezoidal method). Log-transformed date for Cmax/dose and AUC_{0-t}/dose were analyzed using one-way ANOVA regression model to test dose proportionality. Tmax was analyzed using nonparametric test (Kruskal–Wallis test). Volume of distribution (Vd) was calculated using the area under the moment curve following equation: $V_d=A/(AUC\times K_e)$.

For tissue distribution studies, rats in groups of six were intravenously injected with ZYZ-802 (10 mg/kg body weight) and at separate time points (1, 6, 12 and 24 hrs) the animals were sacrificed using carbon dioxide euthanasia. Organs including heart, liver, kidney, spleen and lung were collected and 0.25 g of each organ was homogenized in 1 mL of saline and then centrifuged at 3000 rpm/4°C/10mins. A 20 μL of the supernatant was added to 1 mL of methanol with the internal standard added (0.44 μg/mL Fmoc-S-butyl-cysteine). Following vortexing (1 min) the samples were then centrifuged at 12,000 rpm/4°C/10mins. A 5 μL aliquot of each extract was then used for LC-MS/MS analysis to confirm the presence of ZYZ-802.

H_2S Measurement

H_2S levels modulated by ZYZ-802, DP-ZYZ-802 and SA-ZYZ-802 were evaluated in the plasma and tissues of treated animals. In brief, animals were fasted for 12 hrs before and 3 hrs after dosing. In groups of six, rats were intravenously injected with ZYZ-802 or liposomal carrier (10 mg/kg body weight) via the tail vein and at 1, 6, 12 and 24 hrs the animals were sacrificed using carbon dioxide euthanasia. Blood samples were collected in EDTA-containing tubes and tissues including heart, liver, kidney, spleen and lung removed. Samples were further processed according to previously reported methods and H_2S levels determined as described by Tan et al[37] In brief, chromatography was performed using a Waters Acquity UPLC (Milford, MA, USA) equipped with a Kinetex XB-C18 column (50 mm × 2.1 mm, 2.6 μm) from Phenomenex (Torrance, CA, USA). The components were eluted by a gradient of A) 0.08% formic acid in water and B) acetonitrile and the flow rate was 0.6 mL/min. The Waters Acquity UPLC was coupled with an AB Sciex API 5500 triple quadrupole mass spectrometer (Foster City, CA, Canada). Positive ionization mode for electrospray ionization source was used for detection. Data were collected in selected reaction monitoring (SRM) mode using transitions of m/z 415.1 → m/z 223.3 (SDB) and m/z 419.1 → m/z 227.3 (36S-labeled SDB). The data were acquired and processed using AB Sciex Analyst 1.5 Software (Foster City, CA, Canada). The method was validated for different biological matrices, including plasma, tissues (i.e., heart, liver, kidney), and cultured cells. Validation parameters such as selectivity, linearity, precision, accuracy, recovery, matrix effects, and stability were investigated according to the Guidelines for Bioanalytical Method Validation of the Food and Drug Administration (FDA). The concentrations of H_2S were determined using a standard curve.

Animal Model and Experiments

A heart failure model was used as previously reported.[12,38] In brief, animals were anesthetized and connected to an electrocardiograph (ECG) recorder and a tracheal intubation performed. Once the animals were breathing passively, the chest between the third and fourth rib was opened and the left coronary artery was ligated permanently at the left anterior descending (LAD) with a silk thread. Sham surgery was performed but without ligation for the sham control group. An immediate color change in the ischemic area and an ST-segment elevation as determined using electrocardiogram were considered as successful ligation. The chest was

closed and povidone iodine was used to sterilize the skin. After 24 hrs, except the Sham group treated with saline (1 mL/kg/day) (n=8), the surviving animals were randomly divided into four groups with average body weights were similar between the groups: HF treated with saline (1 mL/kg/day) (n=12), HF treated with DP-LP (1 mL/kg/day) (n=12), HF treated with ZYZ-802 (10 mg/kg/day) (n=10), HF treated with DP-ZYZ-802 (10 mg/kg/day) (n=10). All treatments were randomly applied via intravenous tail vein injection for 6 weeks. Following this procedure, cardiac parameters were assessed using echocardiography (Vevo770, Visual Sonic Inc., Toronto, Canada; with a 716 probe). Hereafter, the animals were sacrificed using carbon dioxide euthanasia, heart/body weight ratio and infarct size determination, and histopathology analysis of myocardial fibrosis as previously described.[12] Afterward, samples of 6 rats from each group were randomly selected for the subsequent experiments. All measurements and data analyst were performed by a person blinded to the treatment group.

Biomarker Analysis

Antioxidant and stress markers including the measurement of superoxide dismutase (SOD), glutathione (GSH), malondialdehyde (MDA), TGF-β1 and brain natriuretic peptide (BNP) were measured in serum samples. All measurements were conducted six times independently using commercially available kits in accordance with the manufacturer's instruction (A001-3-2, A006-2-1, A003-1-2, H034 and H166; Nanjing Jiancheng Bioengineering Institute, Nanjing, China) and data are presented as fold change of Sham group to control for unwanted sources of variation.

Immunoblot Analysis

Tissue lysates were prepared using RIPA lysis buffer (Beyotime Biotechnology, Shanghai, China) containing protease and phosphatase inhibitors. Protein concentrations were determined by BCA protein assay kit (Beyotime Institute of Biotechnology, Shanghai, China). Immunoblot was used to determine protein expression levels using standard procedures. Following the transfer of proteins onto polyvinylidene fluoride (PVDF) membranes (Millipore, Billerica, MA) and blocked with 5% BSA (Sigma-Aldrich) for 1 h at 37°C, these were incubated with the respective primary antibodies at 4°C overnight. After several washes with TBST buffer (0.1% Tween 20) the membranes were then incubated with an appropriate peroxidase-conjugated secondary antibody (HRP fluorescent Goat anti-Mouse IgG1 (Thermo Fisher Scientific, Inc, NY, USA; Catalogue number: A-21124, Alexa Fluor 568, 1:10000) or Goat anti-Rabbit IgG (Cell Signaling Technology, Inc, NY, USA; Catalogue number: A-11008, Alexa Fluor 488, 1:10000)) for 2 hr at 37°C. The primary antibodies used were anti-CSE (Santa Cruz Biotechnology, Santa Cruz, CA, USA) mouse mAb (Catalogue number:sc-374249; IgG1, 1:1000); anti-Smad2 (Proteintech Group, Inc, IL, USA) rabbit polyclonal antibody (Catalogue number: 12570-1-AP, IgG, 1:1000); anti-Smad3 (Proteintech Group, Inc, IL, USA) rabbit polyclonal antibody (Catalogue number: 25494-1-AP, IgG, 1:1000); anti-phospho-Smad2 (Cell Signaling Technology, Inc, MA, USA) rabbit mAb (Catalogue number: 8828, Ser465/467, IgG, 1:1000); anti-phospho-Smad3 (Cell Signaling Technology, Inc, MA, USA) rabbit mAb (Catalogue number: 9520, Ser423/425, IgG, 1:1000); anti-CTGF (Proteintech Group, Inc, IL, USA) rabbit polyclonal antibody (Catalogue number: 23936-1-AP, IgG, 1:1000); anti-SMA (Proteintech Group, Inc, IL, USA) rabbit polyclonal antibody (Catalogue number: 55135-1-ig, IgG, 1:1000); anti-MMP2 (Proteintech Group, Inc, IL, USA) mouse mAb (Catalogue number: 66366-1-AP, IgG1, 1:1000); anti-MMP9 (Cell Signaling Technology, Inc, MA, USA) rabbit mAb (Catalogue number: 13667, IgG, 1:1000) anti-Collagen I (Proteintech Group, Inc, IL, USA) rabbit polyclonal antibody (Catalogue number: 14695-1-AP, IgG, 1:1000); anti-GAPDH (Proteintech Group, Inc, IL, USA) rabbit polyclonal antibody (Catalogue number: 10494-1-AP, IgG, 1:1000). Primary Antibodies were diluted in dilution buffer (1% BSA, 0.1% gelatin, 0.5% Triton X-100, 0.05% sodium azide, 0.01M PBS, pH 7.2–7.4) (Beyotime Biotechnology, Shanghai, China). Each final antibody solution was re-used two or three times within 2 weeks. The membranes were probed using an Odyssey two-color infrared laser imaging system (LI-COR Biosciences, Lincoln, NE, USA). The experiments were duplicated to ensure the reliability of the result in six independent sets of data, and representative pictures are shown. The relative intensities of individual protein bands were calculated using ImageJ (NIH) by a person blinded to the treatment group and data are presented as fold change of Sham group to control for unwanted sources of variation.

Statistical Analysis

Results are presented as the mean ± SEM. All experiments have n of at least 5 of group size or were performed at least five times independently. Statistical analyses were performed by GraphPad Prism 5.01 software (GraphPad Software, Inc., San Diego, CA, USA). Statistical differences among the multiple groups were examined using one-way analysis of

variance (ANOVA) or by two-tailed Student's *t*-test. Statistical significance was defined as $P<0.05$.

Results

Characterization of Liposomal ZYZ-802

Two liposomal formulations of ZYZ-802 composed of i) DP-ZYZ-802, (HSPC: Chol: DSPE-PEG: DP; molar ratio =55: 35: 3: 7) and, ii) SA-ZYZ-802, (HSPC: Chol: DSPE-PEG: SA; molar ratio =55: 35: 3: 7) were evaluated in the current work. The physiochemical characteristics of empty liposomes (SA-LP and DP-LP) and carriers containing ZYZ-802 are shown in Table 1 and Figure 1. These nanoparticles were found to maintain a similar spherical particle size of 200nm in diameter when loaded with ZYZ-802, indicating that ZYZ-802 did not alter the particle size of the formulated liposomes. Moreover, the calculated entrapment efficiency showed that the incorporation of ZYZ-802 into each liposome was comparable in each formulation. Additional stability studies conducted at 0, 30 and 60 days indicated that DP-ZYZ-802 was more stable than that of SA-ZYZ-802 with no significant change in particle size and entrapment efficiency across this time course measured with the methods described in the section of materials and methods accordingly (Table 2).

As shown in Figure 2A, the kinetics of ZYZ-802 release from liposomes was determined in vitro following HPLC analysis. Free ZYZ-802 was rapidly released from the dialysis tubing within 30 min. In contrast, both SA-ZYZ-802 and DP-ZYZ-802 demonstrated the prolonged release of ZYZ-802 over 36 hr. This demonstrated that the retention of ZYZ-802 within the liposomal nanoparticles provides a means for the slow-release of ZYZ-802. Based on these observations, the pharmacokinetic profiles for individual liposomes were assessed in vivo.

Pharmacokinetic Profiles of Liposomal ZYZ-802

The pharmacokinetic profiles of both SA-ZYZ-802 and DP-ZYZ-802 were determined in animals following the administration of 10 mg/kg of each liposomal formulation or free ZYZ-802. As shown in Figure 2B, the free drug as well as the two liposomal formulations of ZYZ-802 exhibited simple monoexponential decline over the measured time period. The plasma concentration profiles for each drug were interpreted using a non-compartment method (see Table S1). The maximum observed concentration values (C_{max}) of SA-ZYZ-802 and DP-ZYZ-802 were approximately 5 times higher than that of free ZYZ-802. These results showing that ZYZ-802 was retained within the liposomal formulations rather than been distributed to other tissues. Notably, the terminal phase half-lives for both SA-ZYZ-802 and DP-ZYZ-802 were extended as compared with free ZYZ-802. Indeed, based on the area under the curve data ($AUC_{0-\infty}$), both SA-ZYZ-802 and DP-ZYZ-802 significantly increased the total drug exposure times in animal tissues. However, comparing the two different liposomal formulations, DP-ZYZ-802 was deemed to be superior to SA-ZYZ-802 and had a longer half-life, smaller volume of distribution, reduced apparent clearance and a greater AUC.

Both the liposomal formulations of ZYZ-802 were found to increase the concentration of ZYZ-802 at each time point within the heart, liver, kidney, spleen and lung tissues (Figure 2C–G and Table S2). Maximal accumulation of both liposomal formulations occurred within 1 hr and declined thereafter at the time points 6, 12 and 24 hrs. In each instance, both formulations appeared to be retained in tissues to a greater extent than that of free ZYZ-802. Additional analyses were also conducted to assess whether the tissue distribution rates of each liposomal formulation corresponded to an increase in tissue and plasma H_2S concentrations. As shown in Figure 3A and Table S3, plasma H_2S level for both SA-ZYZ-802 and DP-ZYZ-802 was steadily maintained over several hours as compared to ZYZ-802 alone. Similar patterns of H_2S production in the tissues of animals were also found as shown in Figure 3B–F and Table S4. The two liposomal formulations significantly generated more H_2S than free ZYZ-802 did in all of the tissues at all time points measured. In particular, the H_2S produced in the heart was the most, while the H_2

Table 1 The Physical Properties of Liposomal Formulations Containing ZYZ-802. Five Independent Batches of Each Liposome Formulation Were Evaluated to Calculate the Mean Diameter, Zeta-Potential and Entrapment Efficiency

Physical Properties	DP-ZYZ-802	SA-ZYZ-802	DP-LP	SA-LP
Entrapping efficiency (%)	32.4±3.8	30.3±6.1	/	/
Vesicle diameter (nm)	190.5±5.7	205.4±4.6	191.3±3.9	209.4±2.0
Zeta potential (mV)	−47.2±3.8	45.6±1.7	−45.1±2.5	48.7±4.3

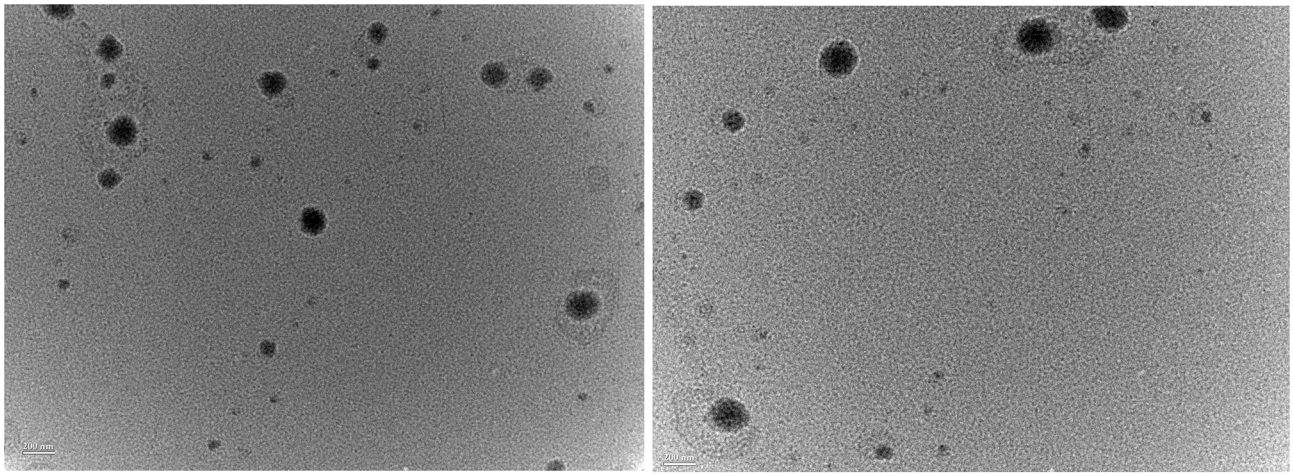

Figure 1 Characterization of liposomal ZYZ-802. Morphological analysis of DP-ZYZ-802 and SA-ZYZ-802 was performed by using Transmission electron micrograph.

S produced in spleen and lung was far lower than any or other tissues.

Since the production of H_2S in tissue seemed contradictory in accordance with ZYZ-802 distribution in tissues, we assumed it should be due to the high expression levels of CSE in heart but not in other tissues. Thus, the expression levels of CSE in different tissues were measured by immunoblots, intending to explain the apparent contradiction. Western blot analysis of tissue extracts indicated that H_2S production rates in tissues corresponded with the protein expression levels of the enzyme CSE (Figure 3G–H). The expression of CSE protein in heart was the highest, which was 23%, 30%, 60% and 60% higher than that in kidney, liver, spleen and lung, respectively.

DP-ZYZ-802 is Cardioprotective in an in vivo Model of Heart Failure

DP-ZYZ-802 was selected for additional analyses based on its pharmacokinetic profiles and stability. Histopathology analysis showed that DP-ZYZ-802 mitigated myocardial fibrosis in heart failure by reducing collagen fiber distribution in HF animals as compared to ZYZ-802 alone (Figure 4A). Triphenyltetrazolium chloride (TTC) staining showed that DP-ZYZ-802 significantly reduced the infarct size in the left ventricle as compared with that of the HF group and was superior to the ZYZ-802 treatment groups (Figure 4B and C). Moreover, the heart/body weight ratio (HW/BW) indicated that DP-ZYZ-802 significantly reduced this ratio (Figure 4D). Typically in this model of heart failure, cardiac functions decrease following left anterior descending coronary artery ligation. As shown in Figure 5 (Supplementary Table S5), at 6 weeks post-surgery, the ejection fraction (EF) values and fractional shortening (FS) values of animals in the HF group were notably lower than those in the Sham group. These effects were reversed in the DP-ZYZ-802 treatment group. In addition, DP-ZYZ-802 significantly reduced left ventricular volume in systole (LVs) and left ventricular internal dimension in systole (LVIDs) and improved left ventricular anterior wall in systole (LVAWs) and left ventricular posterior wall in systole (LVPWs) as compared with the HF group. Taken together the echocardiography results indicated that DP-ZYZ-802 preserved changes in LVs, LVIDs, LVAWs and LVPWs that are caused during heart failure.

Parallel experiments were conducted to determine possible changes in the serum levels of both BNP and TGF-β1. In this instance, both biomarkers were raised approximately 2.9–5.0 fold as compared to the Sham group following the induction of HF. Moreover, DP-ZYZ-802 could effectively restore the levels of both these markers compared with the untreated group (Figure 6). Similarly, in HF group, GSH and SOD activity levels were diminished while lipid peroxidation was elevated. Again in the DP-ZYZ-802 group, GSH and SOD levels were preserved and lipid peroxidation inhibited in animal tissues.

The Effect of DP-ZYZ-802 on TGF-β1/Smad Pathway

Western blot was used to determine protein expression levels of TGF-β1/Smad signaling pathway. As shown in

Table 2 Liposomal Formulations Stability. Five Independent Batches of Liposome Were Stored and Sealed in Sterile Vials at 4°C for 30 and 60 Days. Thereafter, Samples were Taken Out from the vials for Characterization Including Particle Size, and Entrapment Efficiency Evaluation. The stability of liposomal ZYZ-802 Was Assessed in Line with the Original Values Before Storage

Time Period (Day)	DP-ZYZ-802		SA-ZYZ-802	
	Vesicle Diameter (nm)	Entrapping Efficiency (%)	Vesicle Diameter (nm)	Entrapping Efficiency (%)
0	189.0±5.4	30.5±2.0	205.7±5.9	28.6±1.3
30	193.7±4.7	28.9±1.8	252.3±47.4	26.1±1.3*
60	196.1±6.4	27.8±2.0	266.2±47.9*	23.1±0.9*

Notes: *P<0.05 vs 0 Day, calculated by two-tailed Student's t-test

Figure 7B–I, the low protein expression levels of TGF-β1/Smad related proteins in the sham control group are indicative of healthy perfused tissues with no evidence of myocardial fibrosis. In contrast, following the induction of HF a significant increase in the protein expressions' levels of p-Smad2/3, α-SMA, MMP-2/9, CTGF and collagen I were seen; these findings have been consistent with the noted increase in serum TGF-β1 levels. In contrast, the administration of DP-ZYZ-802 effectively reduced the expression of myocardial fibrosis-related proteins. As

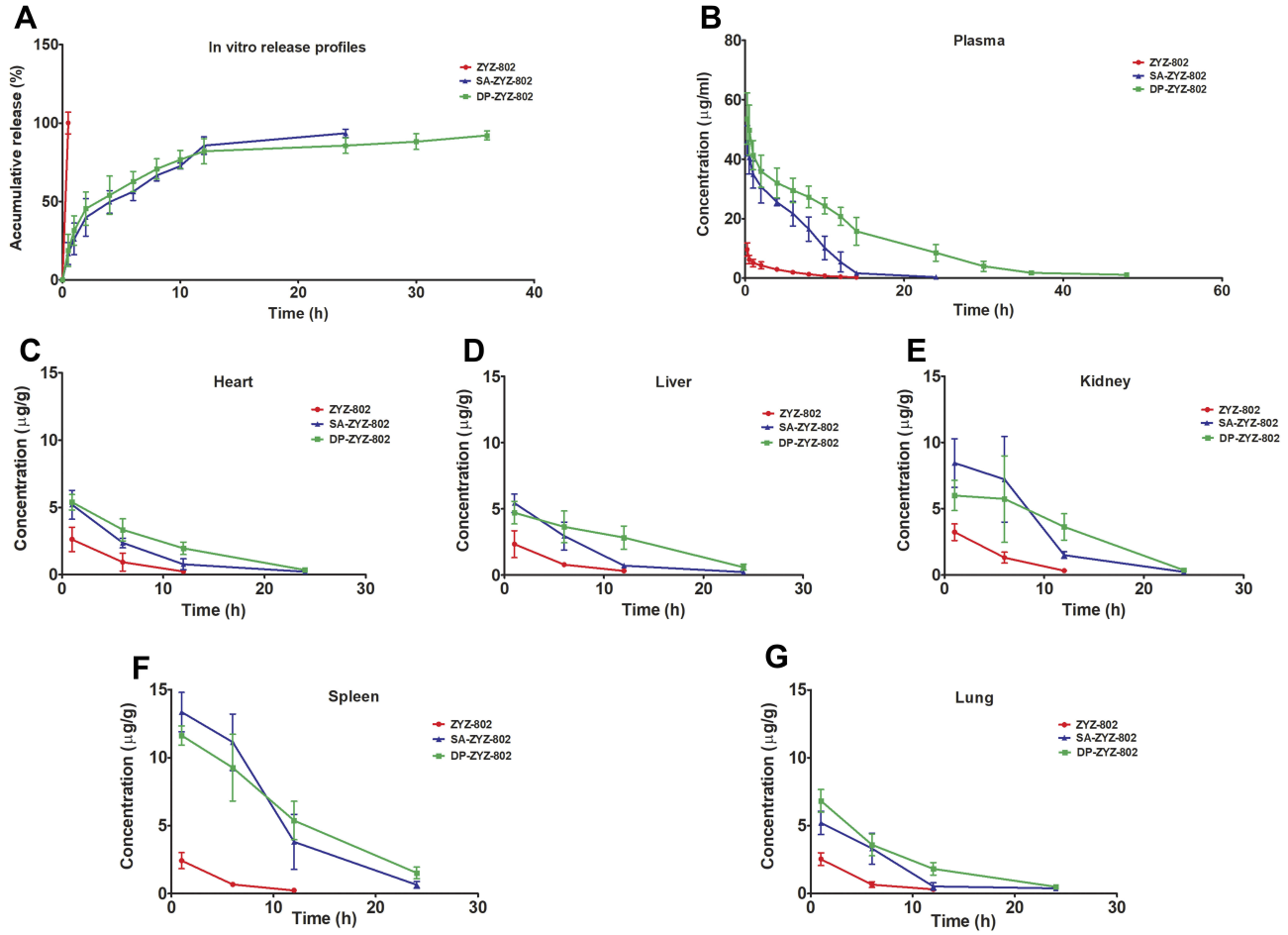

Figure 2 SA-ZYZ-802 and DP-ZYZ-802 prolong the release of ZYZ-802 as determined in vitro and in vivo. (**A**) Representative in vitro release profiles of ZYZ-802, DP-ZYZ-802 and SA-ZYZ-802 measured by HPLC (n=3). (**B**) Plasma concentration–time curves after intravenous injection of ZYZ-802, DP-ZYZ-802 and SA-ZYZ-802 in rats (n=6). (**C**–**G**) Heart, liver, kidney, spleen and lung tissues ZYZ-802 concentrations at different time points (1, 6, 12 and 24 hrs) after intravenous injection of ZYZ-802, DP-ZYZ-802 and SA-ZYZ-802 in rats (n=6). ZYZ-802 plasma and tissue concentration were measured using LC-MS/MS. The graph is representative of six rats per group and the results are expressed as mean ± SEM. Detailed data are listed in Supplementary Tables S1 and S2.

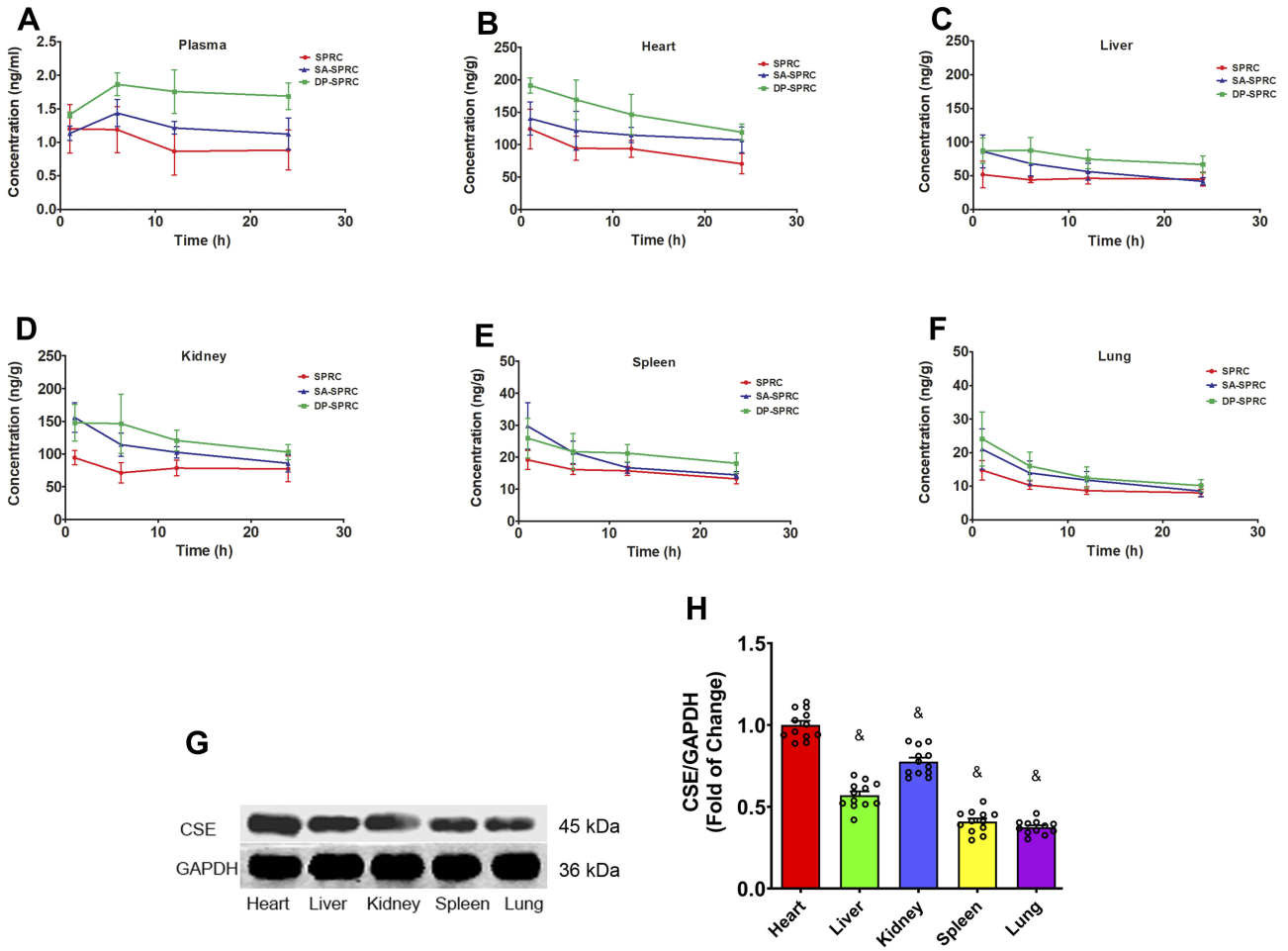

Figure 3 Liposome formulations increased plasma and tissue H_2S concentrations and the protein expression of CSE. (**A**) Plasma H_2S concentrations at different time points after intravenous injection of ZYZ-802, DP-ZYZ-802 and SA-ZYZ-802 in rats, respectively (n=6). The graph is representative of six rats per group and the results are expressed as mean ± SEM. (**B**–**F**) Heart, liver, kidney, spleen and lung tissues H_2S concentrations at different time points after intravenous injection of ZYZ-802, DP-ZYZ-802 and SA-ZYZ-802 in rats, respectively (n=6). After intravenous injection, the concentrations of H_2S gas at 1 hr, 6 hrs, 12 hrs and 24 hrs were measured using LC-MS/MS, respectively. The graph is representative of six rats per group and the results are expressed as mean ± SEM. (**G**–**H**). Finally, the expression of CSE in tissue of animals determined by Western blot (n=6), the blot and bar graph are representative of six independent experiments. Data are presented as fold change of the heart. Results are expressed as mean ± SEM. $^{\&}P<0.05$ vs heart. Detailed data are listed in Supplementary Tables S3 and S4.

compared with the HF group, DP-ZYZ-802 reduced the protein expression levels by 37% for p-Smad2, 32% for p-Smad3, 30% for CTGF, 36% for α-SMA, 30% for MMP-2, 27% for MMP-9 and 24% for collagen I.

The Effect of DP-ZYZ-802 on CSE Expression in Rats

The expression of CSE in the rat heart was analyzed by immunoblots 6 weeks after myocardial infarction. Compared with the HF group, the administration of DP-ZYZ-802 and ZYZ-802 both greatly promoted the expression of CSE (Figure 7A). The CSE expressions of DP-ZYZ-802 group and ZYZ-802 group were 1.7 times and 1.6 times as high as that of HF group or DP-LP group, respectively. More significantly, DP-ZYZ-802 was more effective than ZYZ-802 to elevate CSE expression in HF rats with 23% more expression.

Discussion

It is now widely recognized that H_2S gas plays important roles in many physiological and pathophysiological processes.[39–44] Indeed, in many disease models, tissue H_2S levels are seen to be reduced, and importantly, replenishment of this gas using donor molecules can improve disease outcomes.[45–48] ZYZ-802 is a compound that can alter plasma H_2S levels and the tissue expression of CSE protein.[22,23,49] However, unfavorable clearance of ZYZ-802 in animals hinders its use.[26,27] Therefore, to overcome these limitations and to improve the pharmacokinetic profile of this molecule we have designed and tested two novel

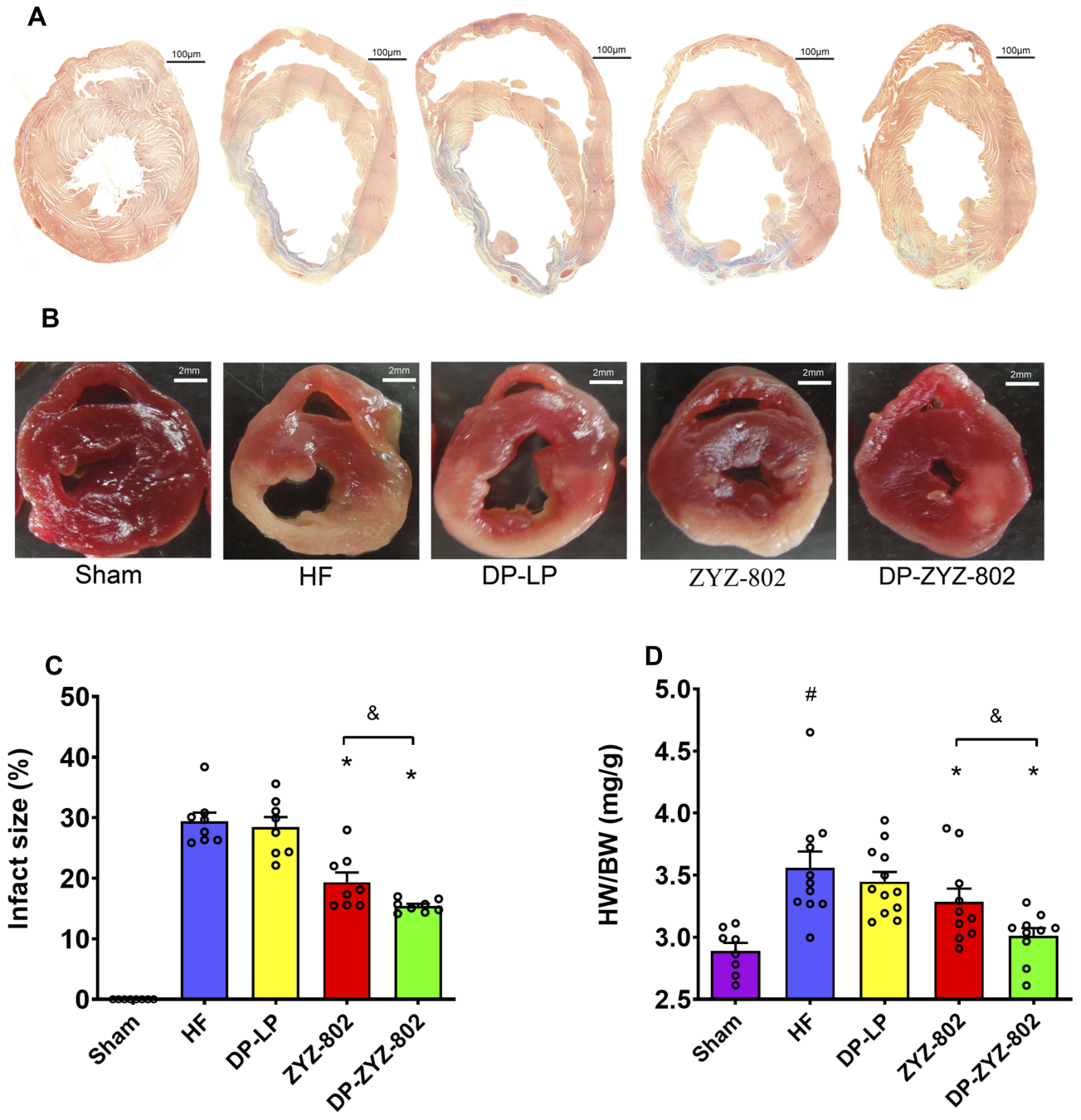

Figure 4 DP-ZYZ-802 decreased cardiac fibrosis, infarct size and HW/BW. (**A**) High-magnification microphotograph of Masson-stained sections from border zones in indicated treatment groups. (**B**) Photograph of infarct size which was determined following staining with 1% triphenyltetrazolium chloride (TTC). (**C**) The infarct sizes were calculated by the ratio of the infarct area and left ventricle. The picture and bar graph are representative of eight rats per group (n=8) and the results are expressed as mean ± SEM. (**D**) Representative statistical analysis of HW/BW with Sham (n=8), HF (n=12), ZYZ-802 (n=10) and DP-ZYZ-802 (n=10). Results are expressed as mean ± SEM, $^{\#}P<0.05$ vs Sham, $^{*}P<0.05$ vs HF, $^{\&}P<0.05$ vs ZYZ-802.

liposomal carrier systems, DP-ZYZ-802 and SA-ZYZ-802. To date, it is widely known that the liposomal delivery of drugs can increase their circulation time, reduce toxicity and enhance the therapeutic efficiency of molecules, and is therefore an attractive system to be employed in drug development.[50]

Traditionally, it is believed that only free drugs not bound to proteins are biologically active. Therefore, the currently available methods measuring the total drug concentration to explain the pharmacokinetics and efficacy of nano-liposomal drugs is insufficient or even could bring misunderstanding, though it remains a difficult problem to be conquered in the research

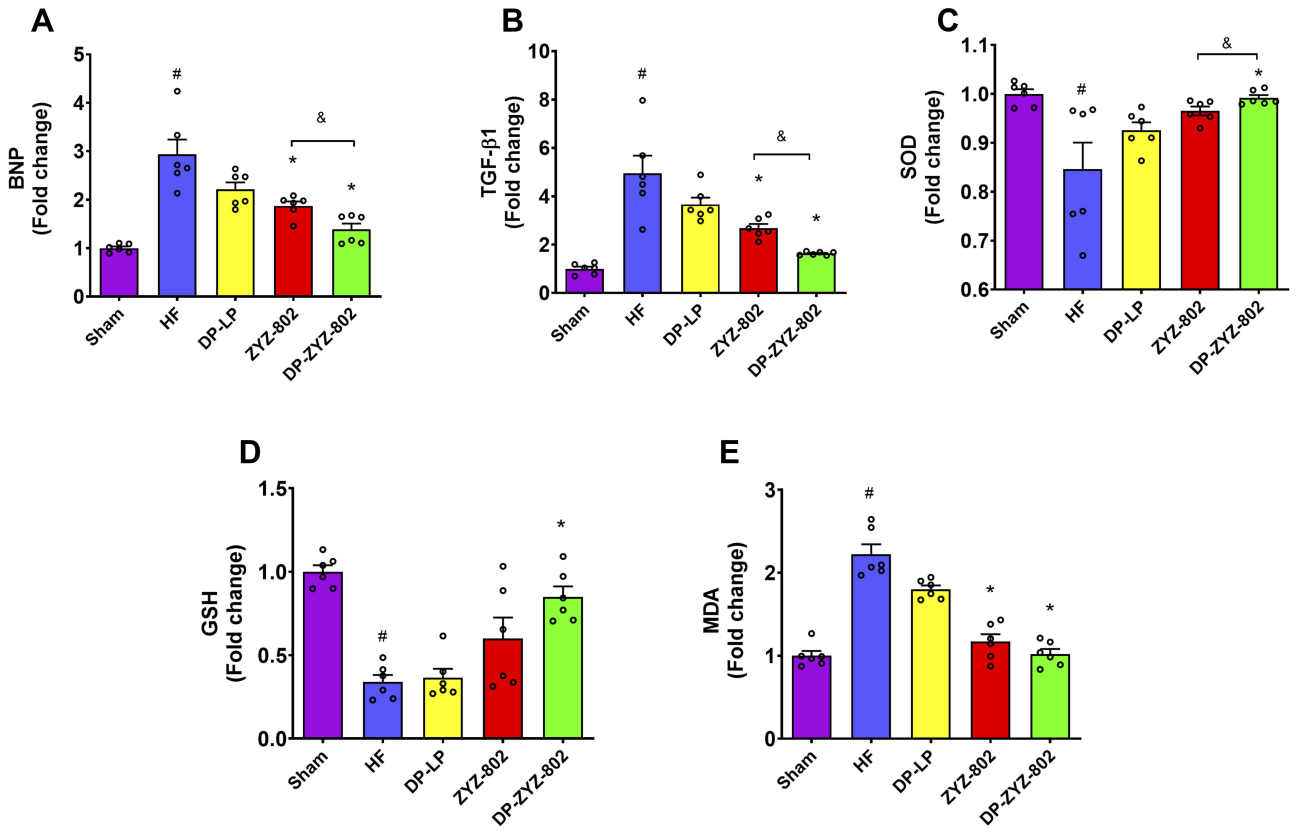

Figure 5 DP-ZYZ-802 improves cardiac function after myocardial infarction. (**A**–**F**) Echocardiographic recordings obtained from a short-axis mid-ventrical view of hearts indicating the changes in the ejection fraction (EF), and fractional shortening (FS), left ventricular internal dimension in systole (LVIDs), left ventricular internal dimension in systole (LVAWs), left ventricular posterior wall in systole (LVPWs) and left ventricular volume in systole (LVs) (n=6). The bar graph is representative of six rats per group and the results are expressed as mean ± SEM, $^{\#}P<0.05$ vs Sham, $^{*}P<0.05$ vs HF, $^{\&}P<0.05$ vs ZYZ-802.

field of liposomal drug delivery to distinguish the amount of free drug and capsulated drug in vivo. In many cases, the enhancement of efficacy of liposomal drugs seems to be due to the direct distribution of the active drug to the target organ by bypassing the unbound form of the active drug. The unbound drug concentrations in encapsulated and unencapsulated form in certain tissue, respectively, should be both useful to provide more accurate information of the PK/PD relationship of the liposomal drugs. Thus, for liposomal drug PK study, in addition to measuring the encapsulated and released drug, it should be more meaningful to distinguish the concentration of drug that is released but not bound to either plasma proteins or tissue proteins. It also has been recommended by the FDA and other agencies as one of the contents for evaluating nanoformulations by determining the drug released without binding to proteins.[51]

In this study, LC-MS/MS method was used to evaluate the pharmacokinetic parameters and tissue distribution profiles of each liposome formulation via the measurements of plasma and tissues ZYZ-802. This method with high sensitivity and specificity has been successfully used to measure ZYZ-802 levels in a broad range of biological matrices, such as blood, plasma, tissues, cells, and enzymes, across different species.[26,36] Pharmacokinetic study showed the accumulation of ZYZ-802 in the kidney and liver. Recent studies suggest that fluorescence dyes are excellent tools to investigate the drug microbiodistribution in the tissue after i.v. administration. However, ZYZ-802 labeled with fluorescence dyes suffer from limitations, firstly, due to their aromatic structure, these molecules are generally poorly soluble in aqueous medium, thus poorly bioavailable. This limited water solubility issue is particularly difficult for the preparation of liposomes. Fluorescence dyes may be degraded or will separate from ZYZ-802 during the preparation of liposomes. For most applications, the stability of dye in tissues is the primary concern. After administration, fluorescence dyes may be separated from ZYZ-802, in this case, the dye concentration in tissues will include fluorescent dye of free and conjugated with ZYZ-802, but may not contain free ZYZ-802 in these tissues. Moreover, dye has narrow excitation bands, small Stokes shifts,

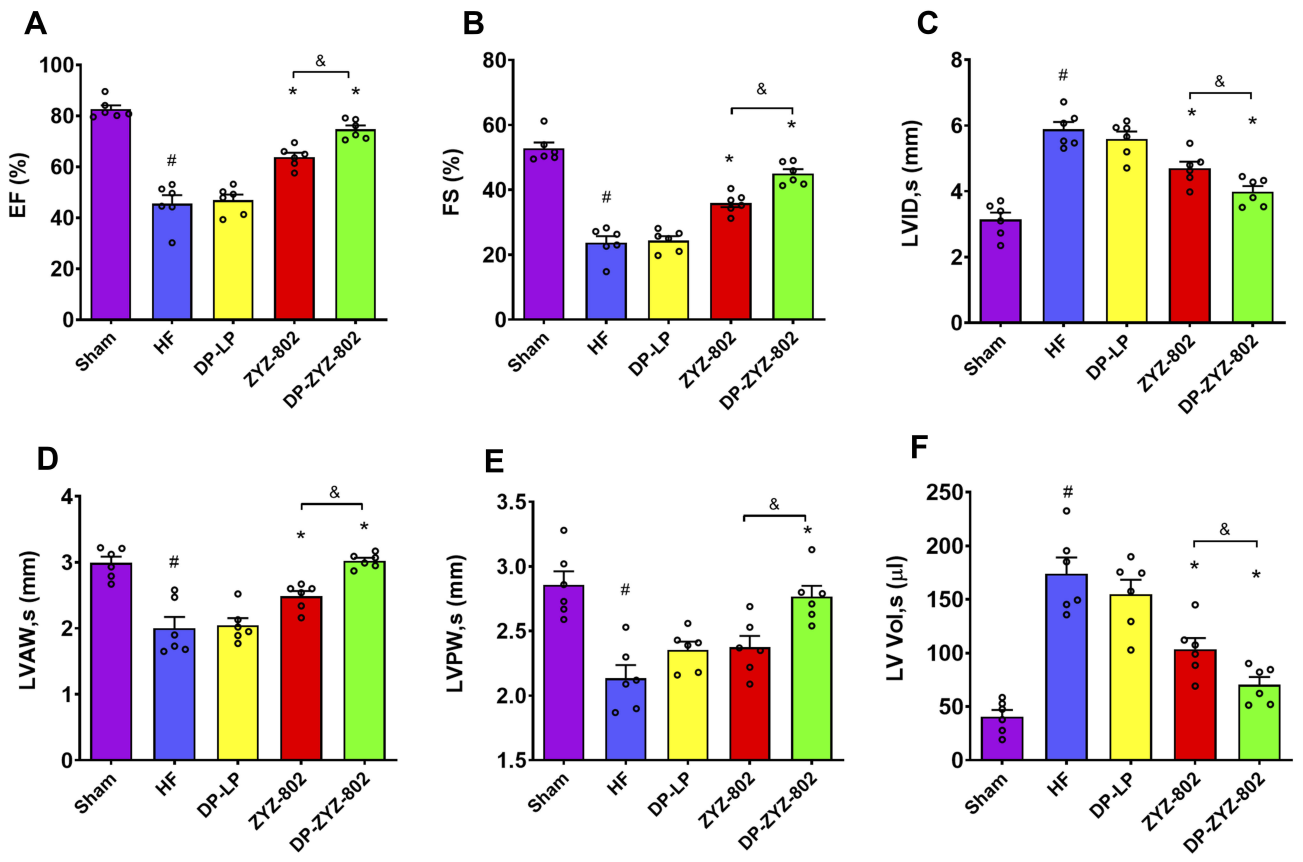

Figure 6 DP-ZYZ-802 alters antioxidant defences and improves cardiac function in myocardial infarction. (**A**–**B**) Serum levels of BNP and TGF-β1 6 weeks after infarction induction (n=6), and (**C**–**E**) serum levels of SOD, GSH and MDA in all groups 6 weeks after infarction (n=6). Data are presented as fold change of Sham group. The bar graph is representative of six independent experiments and the results are expressed as mean ± SEM; $^{\#}P<0.05$ vs Sham, $^{*}P<0.05$ vs HF, $^{\&}P<0.05$ vs ZYZ-802.

autofluorescence, broad fluorescence bands, bleaching and dark states, complication of handling. From these limitations, dye molecules are less attractive for durable, sensitive, accurate quantification and multiplexed imaging.

We have measured the total amount of drugs for liposomal ZYZ-802 pharmacokinetics study and tissue distribution, which is a shortcoming of the current study. Although previous studies have found that the binding rate of ZYZ-802 to plasma proteins is very low in all measured species including human, rat and dog, factors in vivo including physiological, formulation, pathological effects may still affect the binding of ZYZ-802 to plasma and tissue proteins.[26] Instead, rather than assuming the PK profiles and PK/PD relationship of ZYZ-802 simply relying on its protein binding feature from in vitro study, it remains to be necessary to measure the concentrations of both ZYZ-802 that is not directly bound to protein and that is encapsulated when appropriate methods are available in the future.

With this in mind, this study is the first to describe the use of liposomal formulations to deliver an H_2S donor molecule to tissues in order to deliver defined amounts of this gas. In this regard, both liposomal formulations of ZYZ-802 successfully extended the distribution of ZYZ-802 within tissues including the heart, liver, spleen, kidney and lung. Interestingly, liposomal formulation of ZYZ-802 resulted in the highest amount of ZYZ-802 distributing to the spleen. Generally, systematically administered liposomes are mostly taken up by the reticuloendothelial system (RES), which contributes to the major accumulate of liposomal particles in tissue such as spleen and liver because RES is more abundant in these tissues.[52] In contrast, the corresponding produced H_2S was far lower than expected in spleen but it was the highest amount in heart and kidney. Meanwhile, the concentrations of H_2S in spleen and lung did not alter too much at 1hr and 6hrs. The phenomenon seemed somewhat controversy to the ZYZ-802 distribution in tissue, but it was not. Sharing the similar structure of cysteine, ZYZ-802 could increase the expression of CSE and promote the production of H_2S in accordance with our previous study.[25] Recent studies indicated that CSE mainly distributed in heart, kidney and liver but not spleen or lung. Our immunoblot study also demonstrated that CSE mostly expressed in heart and kidney whereas barely expresses in spleen or lung. Although

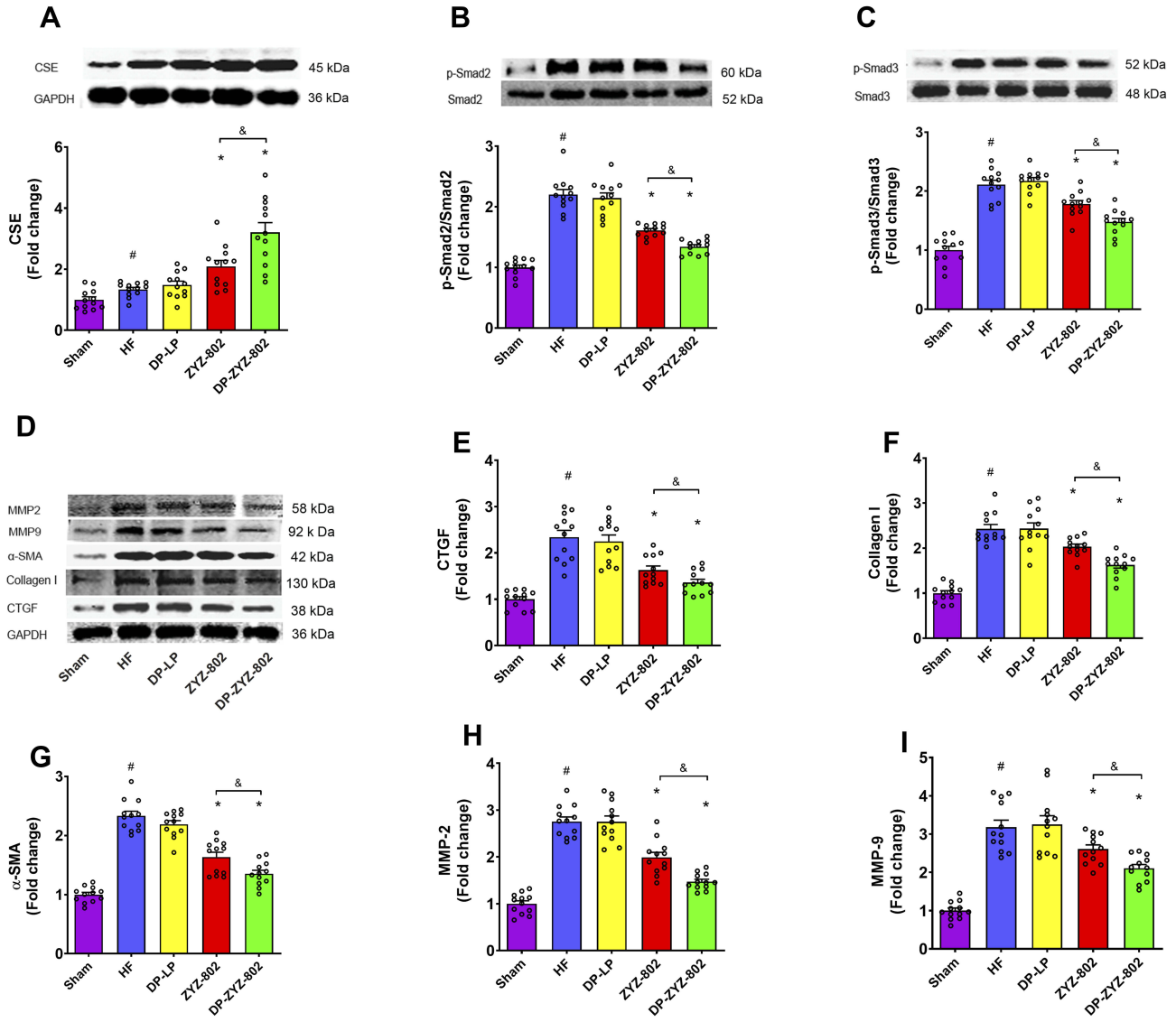

Figure 7 DP-ZYZ-802 increases the expression of the H_2S biosynthetic enzymes CSE in heart tissues and alleviates cardiac fibrosis after myocardial infarction. (**A**) The expression of CSE in the heart following Western blot analysis (n=6). (**B**–**I**) Western blot and statistically analysis indicate that DP-ZYZ-802 decreases the expression of p-Smad2/3, CTGF, Collagen I, α-SMA, MMP-2 and MMP-9 in hearts following myocardial infarction (n=6). The blot and bar graph are representative of six independent experiments. Data are presented as fold change of Sham group. Results are expressed as mean ± SEM, $^{\#}P<0.05$ vs Sham, $^{*}P<0.05$ vs HF, $^{\&}P<0.05$ vs ZYZ-802.

the liposomes increased ZYZ-802 concentration in spleen and lung, the amount of CSE in these two organs was relatively saturated, thus leading to the little difference in H_2S production at 1hr and 6hrs. Likewise, the amounts of ZYZ-802 in lung and liver were comparable to those in heart and kidney, but heart and kidney obviously generated more H_2S.

In accordance with the stability of ZYZ-802 and its poor bioavailability, we intended to improve it from the aspect of liposomal formulation, and our final goal is to solve the problem for its clinical use. However, before it can realize clinical use, there are still several difficulties to be conquered. Firstly, ordinary liposomes composed of phospholipids and cholesterol are pretty sensitive to the destruction of gastric acid and gastrointestinal contents, thus they are easy to be inactivated with low bioavailability. That is also why most liposomes could only be administered intravenously which is not very friendly to chronic diseases. Secondly, lacking of the cell membrane protein skeleton in the phospholipid bilayer membrane, the physical stability is comparatively poor. Since inside the liposomes is liquid, the phospholipid bilayer membrane is highly fluid, and the liposomes are easily deformed and broken both in vitro and in vivo. Additionally, the encapsulation efficiency of the drug in liposomes is generally low,

especially for small water-soluble molecules. Finally, the cost for preparing liposomes is generally higher, and the preparation process and quality control are more complicated.[53,54] Although liposomal drugs have such disadvantages as mentioned above, it is still being explored as an efficient drug delivery approach, especially for potential targeting delivery. Compared with previously developed release formulations for ZYZ-802 vs the Eudragit ® RS30D carrier system,[24,27] these newer liposomal formulations were a much-improved system. Indeed, in this work, in vitro release studies have shown that both liposome formulations have a longer time of release of around 50% of ZYZ-802 and retention time than RS30D. Moreover, nanoparticles delivery system liposome formulation can reach the diseased tissues and taken up by cells more easily than conventional formulation. SA-ZYZ-802 and DP-ZYZ-802 were composed of phospholipid, cholesterol and PEG which are able to integrate with a biological system without eliciting immune response or any negative effects in addition to prolong the circulation of ZYZ-802. Referring to the tissue distribution study, there is still a limitation for the off-target delivery of ZYZ-802 to other tissues. Based on the above points, the creation of liposomal formulation of ZYZ-802 has established a platform for potential specifically targeting the delivery of ZYZ-802 to cardiovascular systems if choosing a proper ligand such as antibodies targeting to vascular endothelial growth factor (VEGF). Since antibody/ligand-targeted liposomal drug delivery systems have shown improved delivery efficiency and reduced off-target effects,[55,56] the utilization of DP-ZYZ-802 or SA-ZYZ-802 for further targeting therapeutic study in cardiovascular disease on the basis of this study should be of great interest, and which is not achievable by the previously reported controlled release RS30D formulation.

The presence of charged groups such as dicetyl phosphate and stearylamine on the liposome surface provides charge to the vesicles, which enhances entrapment efficiency and steric repulsion leading to improved stability. Our study finds that DP-ZYZ-802 is more stable than SA-ZYZ-802 because dicetyl phosphate was more effectively integrate into the phospholipid bilayer membrane of liposome than stearylamine. Furthermore, dicetyl phosphate has long alkyl-chains, resulting in slow drug release, with long lag times. Further characterization of DP-ZYZ-802 showed it to have a more favorable pharmacokinetic profile when measured in plasma and in tissues. As such, subsequent studies have focussed on the use of this carrier in the models of heart failure. Initial in vitro analysis found that DP-ZYZ-802 was cytoprotective in rat embryonic cardiomyocyte cell exposed to hypoxic stress. In this instance, DP-ZYZ-802 preserved cell viability more effectively than SA-ZYZ-802 and ZYZ-802 alone (data not shown). For these reasons, the therapeutic efficacy of DP-ZYZ-802 was further assessed in an in vivo heart failure model. Heart failure is a common syndrome caused by cardiac dysfunction associated with myocardial structural changes due to myocardial infarction (MI), cardiomyopathy and high blood pressure.[56,57] As compared to our previous studies using ZYZ-802, DP-ZYZ-802 was more effective at reducing the HW/BW ratio and in preventing heart fibrosis. Moreover, DP-ZYZ-802 treatment enhanced cardiac indexes including EF, LV, LVID, LVAW and LVPW. Analysis of biomarkers of heart failure showed these were altered in animals receiving DP-ZYZ-802 treatment. Indeed, biomarkers related to cardiac functions, as demonstrated in the preservation of stress markers like SOD and GSH were preserved in tissues following DP-ZYZ-802 treatment, respectively. In addition, in this work, it was also found that plasma levels of BNP were increased following HF induction. Plasma BNP concentrations correlate with the severity of HF and the measurement of serum BNP in patients after myocardial infarction can not only be linked to the infarct size and left ventricular systolic dysfunction, but as a marker of left ventricular remodeling and mortality risk.[59,60] In our study, serum BNP levels increased in HF and were reduced in the DP-ZYZ-802 group. This has been consistent with the echocardiographic findings and the observed cardioprotective effects of DP-ZYZ-802 in our model of heart failure.

Our previous work has demonstrated that ZYZ-802 inhibits TGF-β1 signaling in chronic kidney disease.[61] As such, we next explored whether the cardioprotective effects of ZYZ-802 in HF were due to a similar effect. A large body of evidence indicates that oxidative stress is a common mediator of cardiac damage following HF and that oxidative stress can induce transforming growth factor (TGF-β1) signaling. TGF-β1 is a multifunctional protein that can increase extracellular matrix deposition, can promote the expression of cardiac fibroblasts and increases the synthesis of type I and III collagens.[61–63] Initially, experiments confirmed that DP-ZYZ-802 induces CSE protein expression within the hearts of treated animals. Next, it was shown that TGF-β1 was elevated 6 weeks post-MI induction in our model and that DP-ZYZ-802 suppressed TGF-β1. In the same model, it was also shown using Masson staining specified that DP-ZYZ-802 efficiently reduced the degree of myocardial fibrosis following MI. Interestingly, recent studies have indicated that exogenous H_2S can suppress the expression of MMP-2 and MMP-9, via the inhibition of the TGF-β1/Smad signaling

pathway.[65] Since DP-ZYZ-802 can increase endogenous H_2S gas concentration, it seems reasonable that this molecule is also involved in the suppression of TGF-β1/Smad signaling in our model. Indeed, raised H_2S concentrations in both plasma and tissues, coupled with the increased expression of CSE protein in heart tissues would suggest this to be the case. Accordingly, the expressions of fibrotic proteins in cardiac tissues were determined using Western blot analysis. Consequently, following heart failure, phosphorylated Samd2/3 was found to increase in the heart of rats following MI induction along with the expressions of MMP-2/9, CTGF, α-SMA and collagen I. It could be due to the elevated levels of TGF-β1 thereby activated TGF-β1/Smad. The administration of DP-ZYZ-802 was able to attenuate the expression of p-Smad2/3, and thereby reduce the expression of MMP-2/9, CTGF, α-SMA and collagen I. This finding demonstrates that one of the mechanisms by which DP-ZYZ-802 prevents myocardial fibrosis is likely via an H_2S, TGF-β1/Smad mediated mechanism.

Conclusion

In summary, liposomal formulations have been designed to deliver the cardioprotective agent, ZYZ-802. These carriers offered prolonged maintenance of the endogenous H_2S concentration within animal tissues and had improved pharmacokinetic properties as compared to the parental molecule. In vivo, DP-ZYZ-802 had improved tissue distribution and caused a significant increase and sustained the production of H_2S gas in heart tissues. Moreover, it was also demonstrated that DP-ZYZ-802 had significant therapeutic effects in HF and could inhibit the TGF-β1/Smad signaling pathway. Further preclinical studies based on the use of the identified formulations are warranted.

Abbreviations

3-MST, 3-mercaptopyruvate sulfur transferase; BNP, brain natriuretic peptide; CBS, cystathionine β-synthase; Chol, cholesterol; CTGF, connective tissue growth factor; CSE, cystathionine γ-lyase; DP, dicetylphosphate; ECM, extracellular matrix EF, ejection fraction; FBS, fetal bovine serum; FS, fractional shortening; GSH, glutathione; HF, heart failure; H/R hypoxia/reoxygenation; HSPC, hydrogenated soy phosphatidylcholine; HW/BW, heart/body weight ratio; LC-MS/MS, liquid chromatography-mass spectrometry/mass spectrometry; LVIDs, left ventricular internal dimension in systole; LVIDd, left ventricular internal dimension in diastole LP, liposomal; LVs, left ventricular volume in systole; LVd, left ventricular volume in diastole LVAWs, left ventricular anterior wall in systole; LVAWd, left ventricular anterior wall in diastole LVPWs, left ventricular posterior wall in systole; LVPWd, left ventricular posterior wall in diastole MDA, malondialdehyde; MI, myocardial infarction; MMP-2/9, metalloproteinase-2/metalloproteinase-9; MTT, 3-(4,5-dimethylthiazol-2-yl)-2,5-diphenyltetrazolium bromide PDGF-D, platelet-derived growth factor D; PEG, polyethylene glycol; PEG-DSPE, poly (ethylene glycol)-distearoylphosphatidylethanolamine; SA, stearylamine; SAC, S-allylcysteine; α-SMA, α-smooth muscle actin; Smad, SMAD family member; SOD, superoxide dismutase; SPF, specific pathogen free; SPRC, S-propargyl-cysteine; ZYZ-802; TGF-β1, transforming growth factor β1; TTC, triphenyltetrazolium chloride; VEGF, vascular endothelial growth factor; $AUC_{(0-t)}$, area under the curve, from t=0 to t=48hrs; $AUC_{(0-\infty)}$, area under the curve, from t=0 to infinity; C_{free}, free drug concentration; C_{max}, maximum observed concentration; C_{total}, total concentration; CL, apparent clearance; MRT, mean retention time; V_d, volume of distribution.

Acknowledgments

This work has been supported by grants from Shanghai Committee of Science and Technology of China (No. 19QA1401500, 16431902000), Shanghai Chenguang Program (No. 14CG03), National Natural Science Foundation of China (No. 81402956, 81573421, 81330080), Shanghai Committee of Science and Technology of China (No. 16431902000), Shanghai Pujiang Program from Shanghai Committee of Science and Technology of China (No. 14PJ1401000). The abstract of this paper was presented at the 5th China Pharmaceutical University International Students Academic Innovation Forum as a poster presentation and oral presentation. The abstract was published in the forum programme and abstract book of the 5th China Pharmaceutical University International Students Academic Innovation Forum and is not published elsewhere or under consideration for publication.

Author Contributions

All authors contributed to conception and design, acquisition of data, or analysis and interpretation of data, drafting or revising the article; provided reagents/materials/analysis tools; approved the final manuscript and agree to be accountable for all aspects of the work.

Disclosure

The authors report no conflicts of interest in this work.

References

1. Bazhanov N, Ansar M, Ivanciuc T, Garofalo RP, Casola A. Hydrogen sulfide: a novel player in airway development, pathophysiology of respiratory diseases, and antiviral defenses. *Am J Respir Cell Mol Biol*. 2017;57(4):403–410. doi:10.1165/rcmb.2017-0114TR
2. Chan SJ, Wong PT. Hydrogen sulfide in stroke: protective or deleterious? *Neurochem Int*. 2017;105:1–10. doi:10.1016/j.neuint.2016.11.015
3. Wang R. Physiological implications of hydrogen sulfide: a whiff exploration that blossomed. *Physiol Rev*. 2012;92(2):791–896. doi:10.1152/physrev.00017.2011
4. Shibuya N, Koike S, Tanaka M, et al. A novel pathway for the production of hydrogen sulfide from D-cysteine in mammalian cells. *Nat Commun*. 2013;4:1366. doi:10.1038/ncomms2371
5. Kanagy NL, Szabo C, Papapetropoulos A. Vascular biology of hydrogen sulfide. *Am J Physiol Cell Physiol*. 2017;312(5):C537–C549. doi:10.1152/ajpcell.00329.2016
6. Sivarajah A, Collino M, Yasin M, et al. Anti-apoptotic and anti-inflammatory effects of hydrogen sulfide in a rat model of regional myocardial I/R. *Shock*. 2009;31(3):267–274. doi:10.1097/SHK.0b013e318180ff89
7. Hosoki R, Matsuki N, Kimura H. The possible role of hydrogen sulfide as an endogenous smooth muscle relaxant in synergy with nitric oxide. *Biochem Biophys Res Commun*. 1997;237(3):527–531. doi:10.1006/bbrc.1997.6878
8. Cai WJ, Wang MJ, Moore PK, et al. The novel proangiogenic effect of hydrogen sulfide is dependent on Akt phosphorylation. *Cardiovasc Res*. 2007;76(1):29–40. doi:10.1016/j.cardiores.2007.05.026
9. Szabo C, Papapetropoulos A. Hydrogen sulphide and angiogenesis: mechanisms and applications. *Br J Pharmacol*. 2011;164(3):853–865. doi:10.1111/bph.2011.164.issue-3
10. Tao BB, Liu SY, Zhang CC, et al. VEGFR2 functions as an H2S-targeting receptor protein kinase with its novel Cys1045-Cys1024 disulfide bond serving as a specific molecular switch for hydrogen sulfide actions in vascular endothelial cells. *Antioxid Redox Signal*. 2013;19(5):448–464. doi:10.1089/ars.2012.4565
11. Geng B, Chang L, Pan C, et al. Endogenous hydrogen sulfide regulation of myocardial injury induced by isoproterenol. *Biochem Biophys Res Commun*. 2004;318(3):756–763. doi:10.1016/j.bbrc.2004.04.094
12. Zhu YZ, Wang ZJ, Ho P, et al. Hydrogen sulfide and its possible roles in myocardial ischemia in experimental rats. *J Appl Physiol (1985)*. 2007;102(1):261–268. doi:10.1152/japplphysiol.00096.2006
13. Wang Y, Zhao X, Jin H, et al. Role of hydrogen sulfide in the development of atherosclerotic lesions in apolipoprotein E knockout mice. *Arterioscler Thromb Vasc Biol*. 2009;29(2):173–179. doi:10.1161/ATVBAHA.108.179333
14. Xin H, Wang M, Tang W, et al. Hydrogen sulfide attenuates inflammatory hepcidin by reducing IL-6 secretion and promoting SIRT1-mediated STAT3 deacetylation. *Antioxid Redox Signal*. 2016;24(2):70–83. doi:10.1089/ars.2015.6315
15. Zhou YF, Wu XM, Zhou G, et al. Cystathionine beta-synthase is required for body iron homeostasis. *Hepatology*. 2018;67(1):21–35. doi:10.1002/hep.29499
16. Zhong G, Chen F, Cheng Y, Tang C, Du J. The role of hydrogen sulfide generation in the pathogenesis of hypertension in rats induced by inhibition of nitric oxide synthase. *J Hypertens*. 2003;21(10):1879–1885. doi:10.1097/00004872-200310000-00015
17. Qingyou Z, Junbao D, Weijin Z, et al. Impact of hydrogen sulfide on carbon monoxide/heme oxygenase pathway in the pathogenesis of hypoxic pulmonary hypertension. *Biochem Biophys Res Commun*. 2004;317(1):30–37. doi:10.1016/j.bbrc.2004.02.176
18. Pan LL, Liu XH, Gong QH, Yang HB, Zhu YZ. Role of cystathionine gamma-lyase/hydrogen sulfide pathway in cardiovascular disease: a novel therapeutic strategy? *Antioxid Redox Signal*. 2012;17(1):106–118. doi:10.1089/ars.2011.4349
19. Kashfi K, Olson KR. Biology and therapeutic potential of hydrogen sulfide and hydrogen sulfide-releasing chimeras. *Biochem Pharmacol*. 2013;85(5):689–703. doi:10.1016/j.bcp.2012.10.019
20. Zhao Y, Biggs TD, Xian M. Hydrogen sulfide (H2S) releasing agents: chemistry and biological applications. *Chem Commun (Camb)*. 2014;50(80):11788–11805. doi:10.1039/C4CC00968A
21. Rose P, Whiteman M, Moore PK, Zhu YZ. Bioactive S-alk(en)yl cysteine sulfoxide metabolites in the genus Allium: the chemistry of potential therapeutic agents. *Nat Prod Rep*. 2005;22(3):351–368. doi:10.1039/b417639c
22. Liang YH, Shen YQ, Guo W, Zhu YZ. SPRC protects hypoxia and re-oxygenation injury by improving rat cardiac contractile function and intracellular calcium handling. *Nitric Oxide*. 2014;41:113–119. doi:10.1016/j.niox.2014.05.010
23. Wang Q, Wang XL, Liu HR, Rose P, Zhu YZ. Protective effects of cysteine analogues on acute myocardial ischemia: novel modulators of endogenous H(2)S production. *Antioxid Redox Signal*. 2010;12(10):1155–1165. doi:10.1089/ars.2009.2947
24. Huang C, Kan J, Liu X, et al. Cardioprotective effects of a novel hydrogen sulfide agent-controlled release formulation of S-propargyl-cysteine on heart failure rats and molecular mechanisms. *PLoS One*. 2013;8(7):e69205. doi:10.1371/journal.pone.0069205
25. Kan J, Guo W, Huang C, et al. S-propargyl-cysteine, a novel water-soluble modulator of endogenous hydrogen sulfide, promotes angiogenesis through activation of signal transducer and activator of transcription 3. *Antioxid Redox Signal*. 2014;20(15):2303–2316. doi:10.1089/ars.2013.5449
26. Zheng YT, Zhu JH, Ma G, et al. Preclinical assessment of the distribution, metabolism, and excretion of S-propargyl-cysteine, a novel H2S donor, in Sprague-Dawley rats. *Acta Pharmacol Sin*. 2012;33(6):839–844. doi:10.1038/aps.2012.15
27. Tran BH, Huang C, Zhang Q, et al. Cardioprotective effects and pharmacokinetic properties of a controlled release formulation of a novel hydrogen sulfide donor in rats with acute myocardial infarction. *Biosci Rep*. 2015;35:3. doi:10.1042/BSR20140185
28. Eloy JO, Claro DSM, Petrilli R, et al. Liposomes as carriers of hydrophilic small molecule drugs: strategies to enhance encapsulation and delivery. *Colloids Surf B Biointerfaces*. 2014;123:345–363. doi:10.1016/j.colsurfb.2014.09.029
29. Davis ME, Chen ZG, Shin DM. Nanoparticle therapeutics: an emerging treatment modality for cancer. *Nat Rev Drug Discov*. 2008;7(9):771–782. doi:10.1038/nrd2614
30. Han HD, Byeon Y, Jeon HN, Shin BC. Enhanced localization of anticancer drug in tumor tissue using polyethylenimine-conjugated cationic liposomes. *Nanoscale Res Lett*. 2014;9(1):209. doi:10.1186/1556-276X-9-209
31. Kneidl B, Peller M, Winter G, Lindner LH, Hossann M. Thermosensitive liposomal drug delivery systems: state of the art review. *Int J Nanomedicine*. 2014;9:4387–4398. doi:10.2147/IJN.S49297
32. Liu M, Li M, Wang G, et al. Heart-targeted nanoscale drug delivery systems. *J Biomed Nanotechnol*. 2014;10(9):2038–2062. doi:10.1166/jbn.2014.1894
33. Verma DD, Levchenko TS, Bernstein EA, Mongayt D, Torchilin VP. ATP-loaded immunoliposomes specific for cardiac myosin provide improved protection of the mechanical functions of myocardium from global ischemia in an isolated rat heart model. *J Drug Target*. 2006;14(5):273–280. doi:10.1080/10611860600763103
34. Takahama H, Minamino T, Asanuma H, et al. Prolonged targeting of ischemic/reperfused myocardium by liposomal adenosine augments cardioprotection in rats. *J Am Coll Cardiol*. 2009;53(8):709–717. doi:10.1016/j.jacc.2008.11.014
35. Care NRCU, Animals AUOL. Guide for the Care and Use of Laboratory Animals. 2011.

36. Zheng Y, Liu H, Ma G, et al. Determination of S-propargyl-cysteine in rat plasma by mixed-mode reversed-phase and cation-exchange HPLC-MS/MS method and its application to pharmacokinetic studies. *J Pharm Biomed Anal*. 2011;54(5):1187–1191. doi:10.1016/j.jpba.2010.11.027
37. Tan B, Jin S, Sun J, et al. New method for quantification of gasotransmitter hydrogen sulfide in biological matrices by LC-MS/MS. *Sci Rep*. 2017;7:46278. doi:10.1038/srep46278
38. Calvert JW, Elston M, Nicholson CK, et al. Genetic and pharmacologic hydrogen sulfide therapy attenuates ischemia-induced heart failure in mice. *Circulation*. 2010;122(1):11–19. doi:10.1161/CIRCULATIONAHA.109.920991
39. Kolluru GK, Shen X, Bir SC, Kevil CG. Hydrogen sulfide chemical biology: pathophysiological roles and detection. *Nitric Oxide*. 2013;35:5–20. doi:10.1016/j.niox.2013.07.002
40. Liu YH, Lu M, Hu LF, et al. Hydrogen sulfide in the mammalian cardiovascular system. *Antioxid Redox Signal*. 2012;17(1):141–185. doi:10.1089/ars.2011.4005
41. Mustafa AK, Sikka G, Gazi SK, et al. Hydrogen sulfide as endothelium-derived hyperpolarizing factor sulfhydrates potassium channels. *Circ Res*. 2011;109(11):1259–1268. doi:10.1161/CIRCRESAHA.111.240242
42. Szabo C, Ransy C, Modis K, et al. Regulation of mitochondrial bioenergetic function by hydrogen sulfide. Part I. Biochemical and physiological mechanisms. *Br J Pharmacol*. 2014;171(8):2099–2122. doi:10.1111/bph.12369
43. Tang G, Yang G, Jiang B, et al. H(2)S is an endothelium-derived hyperpolarizing factor. *Antioxid Redox Signal*. 2013;19(14):1634–1646. doi:10.1089/ars.2012.4805
44. Yin WL, He JQ, Hu B, Jiang ZS, Tang XQ. Hydrogen sulfide inhibits MPP(+)-induced apoptosis in PC12 cells. *Life Sci*. 2009;85(7–-8):269–275. doi:10.1016/j.lfs.2009.05.023
45. Mani S, Untereiner A, Wu L, Wang R. Hydrogen sulfide and the pathogenesis of atherosclerosis. *Antioxid Redox Signal*. 2014;20(5):805–817. doi:10.1089/ars.2013.5324
46. Zhao H, Lu S, Chai J, et al. Hydrogen sulfide improves diabetic wound healing in ob/ob mice via attenuating inflammation. *J Diabetes Complications*. 2017;31(9):1363–1369. doi:10.1016/j.jdiacomp.2017.06.011
47. Shimizu Y, Polavarapu R, Eskla KL, et al. Hydrogen sulfide regulates cardiac mitochondrial biogenesis via the activation of AMPK. *J Mol Cell Cardiol*. 2018;116:29–40.
48. Guan Q, Wang X, Gao L, et al. Hydrogen sulfide suppresses high glucose-induced expression of intercellular adhesion molecule-1 in endothelial cells. *J Cardiovasc Pharmacol*. 2013;62(3):278–284. doi:10.1097/FJC.0b013e31829875ef
49. Wu WJ, Jia WW, Liu XH, et al. S-propargyl-cysteine attenuates inflammatory response in rheumatoid arthritis by modulating the Nrf2-ARE signaling pathway. *Redox Biol*. 2016;10:157–167. doi:10.1016/j.redox.2016.08.011
50. Wagner A, Vorauer-Uhl K. Liposome technology for industrial purposes. *J Drug Deliv*. 2011;2011:591325. doi:10.1155/2011/591325
51. Stern ST, Martinez MN, Stevens DM. When is it important to measure unbound drug in evaluating nanomedicine pharmacokinetics? *Drug Metab Dispos*. 2016;44(12):1934–1939. doi:10.1124/dmd.116.073148
52. Allen TM, Cullis PR. Liposomal drug delivery systems: from concept to clinical applications. *Adv Drug Deliv Rev*. 2013;65(1):36–48. doi:10.1016/j.addr.2012.09.037
53. Gabizon A, Shmeeda H, Horowitz AT, Zalipsky S. Tumor cell targeting of liposome-entrapped drugs with phospholipid-anchored folic acid-PEG conjugates. *Adv Drug Deliv Rev*. 2004;56(8):1177–1192. doi:10.1016/j.addr.2004.01.011
54. Knop K, Hoogenboom R, Fischer D, Schubert US. Poly(ethylene glycol) in drug delivery: pros and cons as well as potential alternatives. *Angew Chem Int Ed Engl*. 2010;49(36):6288–6308. doi:10.1002/anie.200902672
55. Mann AP, Bhavane RC, Somasunderam A, et al. Thioaptamer conjugated liposomes for tumor vasculature targeting. *Oncotarget*. 2011;2(4):298–304. doi:10.18632/oncotarget.v2i4
56. Mao Y, Wang J, Zhao Y, et al. A novel liposomal formulation of FTY720 (fingolimod) for promising enhanced targeted delivery. *Nanomedicine-Uk*. 2014;10(2):393–400. doi:10.1016/j.nano.2013.08.001
57. Hunt SA, Baker DW, Chin MH, et al. ACC/AHA guidelines for the evaluation and management of chronic heart failure in the adult: executive summary. *J Heart Lung Transplant*. 2002;21(2):189–203. doi:10.1016/S1053-2498(01)00776-8
58. Wencker D, Chandra M, Nguyen K, et al. A mechanistic role for cardiac myocyte apoptosis in heart failure. *J Clin Invest*. 2003;111(10):1497–1504. doi:10.1172/JCI17664
59. Cowie MR. BNP-guided therapy for chronic heart failure: anything more than just an attractive concept? *Eur Heart J*. 2014;35(23):1507–1509. doi:10.1093/eurheartj/ehu134
60. Tsutamoto T, Tanaka T, Sakai H, et al. Beneficial effect of perindopril on cardiac sympathetic nerve activity and brain natriuretic peptide in patients with chronic heart failure: comparison with enalapril. *Circ J*. 2008;72(5):740–746. doi:10.1253/circj.72.740
61. Qian X, Li X, Ma F, et al. Novel hydrogen sulfide-releasing compound, S-propargyl-cysteine, prevents STZ-induced diabetic nephropathy. *Biochem Biophys Res Commun*. 2016;473(4):931–938. doi:10.1016/j.bbrc.2016.03.154
62. Chen MM, Lam A, Abraham JA, Schreiner GF, Joly AH. CTGF expression is induced by TGF- beta in cardiac fibroblasts and cardiac myocytes: a potential role in heart fibrosis. *J Mol Cell Cardiol*. 2000;32(10):1805–1819. doi:10.1006/jmcc.2000.1215
63. Deten A, Holzl A, Leicht M, Barth W, Zimmer HG. Changes in extracellular matrix and in transforming growth factor beta isoforms after coronary artery ligation in rats. *J Mol Cell Cardiol*. 2001;33(6):1191–1207. doi:10.1006/jmcc.2001.1383
64. Leask A. Potential therapeutic targets for cardiac fibrosis: tGFbeta, angiotensin, endothelin, CCN2, and PDGF, partners in fibroblast activation. *Circ Res*. 2010;106(11):1675–1680. doi:10.1161/CIRCRESAHA.110.217737
65. Sun L, Jin H, Sun L, et al. Hydrogen sulfide alleviates myocardial collagen remodeling in association with inhibition of TGF-beta/Smad signaling pathway in spontaneously hypertensive rats. *Mol Med*. 2015;20:503–515. doi:10.2119/molmed.2013.00096

International Journal of Nanomedicine Dovepress

Publish your work in this journal

The International Journal of Nanomedicine is an international, peer-reviewed journal focusing on the application of nanotechnology in diagnostics, therapeutics, and drug delivery systems throughout the biomedical field. This journal is indexed on PubMed Central, MedLine, CAS, SciSearch®, Current Contents®/Clinical Medicine, Journal Citation Reports/Science Edition, EMBase, Scopus and the Elsevier Bibliographic databases. The manuscript management system is completely online and includes a very quick and fair peer-review system, which is all easy to use. Visit http://www.dovepress.com/testimonials.php to read real quotes from published authors.

Submit your manuscript here: https://www.dovepress.com/international-journal-of-nanomedicine-journal